# Synthesis of Zn/Mg Oxide Nanoparticles and Its Influence on Sulfur Vulcanization

**Manuel Guzmán,[1,2] Guillermo Reyes,[2] Núria Agulló,[1,2] Salvador Borrós[1,2]**

[1]*Grup d'Enginyeria de Materials, Institut Químic de Sarrià, Universitat Ramon Llull, Via Augusta 390, Barcelona 080017, Spain*
[2]*Industrial Engineering Department, Institut Químic de Sarrià, Universitat Ramon Llull, Via Augusta 390, Barcelona 080017, Spain*

Received 5 March 2010; accepted 31 May 2010
DOI 10.1002/app.32885
Published online 26 August 2010 in Wiley Online Library (wileyonlinelibrary.com).

**ABSTRACT:** To reduce the ZnO levels in rubber compounds, mixed metal oxide nanoparticles of zinc and magnesium ($Zn_{1-x}Mg_xO$) have been synthesized and used as activator. The aim is to obtain better curing properties due to its nanosize and to take advantage of the behavior of both ZnO and MgO in sulfur vulcanization. The model compound vulcanization approach with squalene as a model molecule for NR and CBS as accelerator has been used to study the role of the mixed metal oxide along the reaction. The results found show that with $Zn_{1-x}Mg_xO$ nanoparticles the reaction of CBS becomes faster, higher amounts of MBT are formed at shorter reaction times, and the consumption of sulfur occurs faster in comparison with standard ZnO. Furthermore and more important, an increased crosslink degree calculated as the total amount of crosslinked squalene is obtained. All these findings indicate that $Zn_{1-x}Mg_xO$ is a promising candidate to reduce the ZnO levels in rubber compounds. © 2010 Wiley Periodicals, Inc. J Appl Polym Sci 119: 2048–2057, 2011

**Key words:** nanoparticles; rubber; vulcanization; zinc oxide; mixed metal oxides

## INTRODUCTION

Zinc oxide is a widely used compound in rubber industry because of the excellent properties that shows as activator for sulfur vulcanization. The tire industry remains the largest single market for ZnO, consuming more than half of the total worldwide demand of 1,200,000 metric tons.[1] Traditionally, ZnO is used in rubber formulations in concentrations of 3–8 parts per hundred rubber (phr). The effects of ZnO can be summarized in Ref. 2:

- Increase in vulcanization rate and crosslink efficiency.
- Filler and scavenger.
- Improvement of abrasion resistance.
- Improvement of dynamic properties.
- Improved ageing properties in peroxide cure.

The mechanism of accelerated sulfur vulcanization has been extensively studied. The first step consists on the reaction of the accelerator with sulfur to give active sulfurating agents, Ac-$S_z$-Ac. The mechanism when *N*-cyclohexylbenzothiazole-2-sulfenamide (CBS) is the accelerator is depicted in Scheme 1. Initially, CBS decomposes and the S—N bond of the accelerator is cleaved forming 2-mercaptobenzothiazole (MBT) and cyclohexanamine. Then, the reaction between MBT and another molecule of CBS results in the formation of 2,2′-dithiobenzothiazole (MBTS) that reacts with sulfur yielding in the active sulfurating agents. Borrós and Agulló[3] demonstrated that ZnO, which is usually described as a catalyst for the breaking down of the accelerator, is necessary but not enough to cause the decomposition of the sulfenamide. These authors proved that this compound is initially formed from the direct interaction between the accelerator and the double bonds of the hydrocarbon chain.

The next step in the vulcanization process is the formation of the rubber-bound intermediate compound, *R*-$S_y$-Ac, by the reaction of the active sulfurating agents with the rubber hydrocarbon chain. Finally, the rubber polysulphides react, either directly or through an intermediate, to give crosslinks, *R*-$S_x$-R.

From the mechanistic point of view, the several functions of ZnO in different stages of vulcanisation are as follows:

- The initial scorch reactions proceed faster.
- The crosslinking reactions proceed with a better control and with a better distribution of sulfur in the polymer network.
- Change in crosslink distribution: the crosslinks contain less sulfur atoms, but the number of crosslinks is higher (crosslink density).

*Correspondence to:* S. Borrós (salvador.borros@iqs.url.edu).

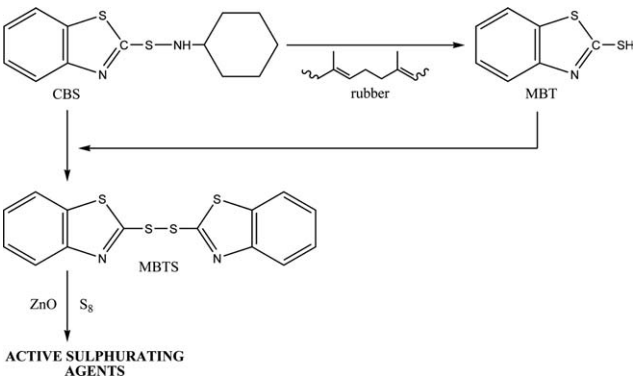


**Scheme 1** Formation of active sulfurating agents. Mechanism proposed by Borrós and Agulló.[3]

Despite its superior characteristics, there is an increased concern about the environmental effects that zinc oxide causes. Over the years, lower levels of zinc have been tried to decrease its impact and to minimize the production costs. Furthermore, different approaches have been considered for reducing zinc levels. Between all the alternatives proposed, the use of nanosized ZnO particles with high surface area seems to be promising. Bhowmick and coworkers[4,5] studied the effect of ZnO nanoparticles (50 nm) as cure activator in natural rubber (NR), acrylonitrile-butadiene rubber (NBR), and polychloroprene rubber (CR). They found that the maximum torque value increased and the tensile strength was improved significantely. An increase in crosslinking density and a decrease in the swelling ratio were also found.

Joseph and coworkers[6] found that a low dosage of zinc oxide nanoparticles was enough to give equivalent curing and mechanical properties to NR compared to the one containing a higher dosage of conventional zinc oxide.

Parasiewicz and coworkers[7] investigated the effect of different concentrations of ZnO nanoparticles (100 nm) in isoprene rubber (IR) and styrene-butadiene rubber (SBR). They reported that the reduction of ZnO content to 2 phr resulted in shortening of scorch and optimal vulcanization time but the extent of cure was on the same level. The mechanical properties did not vary significantly when using active or standard ZnO. They attributed the small differences between active ZnO and standard ZnO despite its nine times higher specific surface area to the poorer dispersion of the active ZnO and its tendency to form agglomerates.

Chapman[8] examined the impact of high surface area/small particle size zinc oxide in sulfur vulcanization of NR, EPDM, and SBR. It was found that the use of more active forms of zinc oxide did not substantially reduce further the minimum zinc content that can be achieved with conventional zinc oxide, contrary to other suggestions in the literature. However, the dispersion of high surface area ZnO during mixing was found to be significantly better, which could enable low levels of this zinc oxide to be used in industry with more confidence. It was also reported a slight increase of scorch delay.

Noordermeer and coworkers[9] studied the influence of active ZnO (0.1–0.4 μm) and nano-ZnO (20–40 nm) in SBR. Their results are similar to those mentioned earlier for active ZnO; it apparently had a negligible influence on the cure characteristics and physical properties. However, they concluded that only one-tenth of the amount of nano-ZnO is necessary to achieve the same cure characteristics in comparison with conventional ZnO.

Thus, the use of ZnO nanoparticles as activator for sulfur accelerated vulcanization seems a good proposal for reducing the zinc levels despite some contradictory results previously explained.

Another approach considered for reducing zinc levels is the used of zinc complexes. Several proposals have been suggested: zinc complex with 18-crown-6-ether,[7,10] zinc monomethacrylate,[11] the so-called ZnClay,[12,13] zinc stearate, zinc-2-ethylhexanoate, zinc borate, and zinc-*m*-glycerolate.[14] Although some proposals look very interesting, the limited amount of data available and their limitation in most cases only to some types of rubber compounds have restricted their industrial application.

Finally, using other oxides as activators for rubber vulcanization was also studied as alternative to ZnO. Several metal oxides have been used, CaO, MgO, CdO, CuO, PbO, and NiO. Among them, MgO is the most promising candidate.

Borrós and coworkers[15] studied the role of MgO using the model compound vulcanization (MCV) approach with squalene as a model molecule for NR and CBS. They found that the breakdown of the accelerator occurs faster with MgO but higher crosslink degree is obtained with ZnO.

These results are in good agreement with those found by Noordermeer and coworkers[16] using model molecules and *N*-t-butylbenzothiazole-2-sulfenamide (TBBS). They observed that when using MgO the accelerator dissociates very rapidly and crosslinked products are formed. However, the crosslinks are formed to a higher extent with ZnO.

These authors also compared the effect of different metal oxides with EPDM[9] and SBR.[9,13] In EPDM with tetramethylthiuram disulphide (TMTD) as accelerator, none of the metal oxides studied was as active as ZnO. In SBR with TBBS as accelerator, the substitution of ZnO by MgO did not cause large effects on the cure and physical properties. The scorch times were comparable with the reference compound with ZnO, but the rates of cure were to a certain extent lower. The extent of crosslinking of

the compounds was slightly lower although, in contrast with ZnO, at longer vulcanization times no decrease or reversion was observed.

In another paper by Borrós and coworkers[17] the effect of different activators by MCV using microwave heating was studied. They concluded that both zinc oxide and magnesium oxide react with similar kinetics when microwave emission is applied. A synergetic effect between magnesium and zinc oxides was observed when using a mixture of them. This effect can also be observed with conventional heating, in the reaction kinetics, although they found it was enhanced when using microwaves.

Vega[18] in her thesis found that when mixing ZnO and MgO in NR using CBS as accelerator, MgO cures with good kinetics in comparison with ZnO but the crosslink density obtained is much lower. MgO seemed to have more affinity for sulfur than ZnO because of its ability to form active sulfurating agents more quickly. However, these MgO intermediates were not able to progress to final crosslinks with the same ability than ZnO active sulfurating agents. Therefore, when working with mixtures of both oxides, MgO competes with ZnO to react with sulfur, and due to the higher affinity of MgO for sulfur, it takes up part of the sulfur which cannot react to form final crosslinks.

In summary, although there is a lack of agreement respect the effect of MgO, mainly caused by the differences in the vulcanising system, magnesium is a non-heavy metal oxide that forms active sulfurating agents. However, the crosslink level achieved is lower than that obtained with zinc oxide.

As it has been illustrated earlier, although magnesium oxide cannot be considered to substitute zinc oxide, it has been proven to be a potential substance to reduce ZnO. Its ability to form active sulfurating agents even faster than ZnO provides a not only the possibility to reduce the zinc oxide levels in rubber compounds but to improve the cure characteristics. However, it affects significantly the crosslink degree, which prevents its use in vulcanization.

In this article, a new approach to overcome the problems between ZnO and MgO is presented. It consists in the development of a new activator based in the mixture of both oxides at nanoscale. The new activator is nanometer-sized mixed metal oxide (MMO) of zinc and magnesium ($Zn_{1-x}Mg_xO$) with very precise stoichiometry prepared by a polymer-based method. In this activator, magnesium is incorporated into the ZnO structure and this inclusion is presumed to show a better performance. The aim is to gain benefit from the two different approaches indicated before: to obtain better curing properties due to its nanosize and to take advantage of the behavior of both ZnO and MgO in sulfur vulcanization.

## EXPERIMENTAL

### Materials

Poly (acrylic acid) (PAA) (poly (acrylic acid) partial sodium salt solution, average $Mw \sim 5000$, 50 wt % in $H_2O$), magnesium nitrate hexahydrate, $Mg(NO_3)_2{\cdot}6H_2O$, zinc nitrate hexahydrate, $Zn(NO_3)_2{\cdot}6H_2O$, and ammonium hydroxide (30 wt %) were obtained from Sigma-Aldrich. Squalene (Fluka, 97 %), sulfur (Julio Cabrero & Cia, S.L.), CBS (Flexsys), zinc oxide (Zincsa), and stearic acid (Calià & Parés) were used for the model compound studies.

### Synthesis of zinc/magnesium oxide ($Zn_{1-x}Mg_xO$) nanoparticles

Zinc/Magnesium oxide nanoparticles were prepared following the method reported by Wegner and coworkers[19] Basically, the method consists on the preparation of a polymer/metal salt complex that is water-soluble, its purification by precipitation/redissolution cycles and finally the calcination of the dried purified complex to give nanosized particles.

The polymer used to form the polymer/metal salt complex is poly (acrylic acid) that is obtained by freeze drying (CRYODOS, Telstar) from a poly (acrylic acid) partial sodium salt solution. Magnesium nitrate hexahydrate and zinc nitrate hexahydrate are the starting materials and were used as received.

The method for obtaining $Zn_{1-x}Mg_xO$ nanoparticles is as follows. A certain amount of poly(acrylic acid) and $Zn(NO_3)_2{\cdot}6H_2O$ are dissolved in water. At least a fourfold molar excess of carboxylic groups compared to zinc was chosen. Once it is dissolved, nitrogen is bubbled through the solution for about 10 min to remove carbon dioxide. Then, ammonium hydroxide is added dropwise to adjust the pH to 7. The reaction mixture is concentrated in a heating magnetic stirrer. The residual viscous liquid is dropped into acetone and a colorless precipitate is formed. This precipitate is collected by centrifugation, washed with acetone, and dried at 40°C in vacuum.

This material is dissolved again in water and mixed with a solution of the desired amount of magnesium nitrate. The pH is also adjusted to 7 with ammonia. The mixed solution is concentrated and then poured dropwise into acetone. The precursor material, a polymer/metal salt complex, is collected by centrifugation, washed with acetone, and dried in vacuum.

Following, it is milled into a fine powder and then calcined in a temperature-controlled oven under air flow at a heating rate of 5°C/min to 550°C. The

**TABLE I**
**Model Compound Vulcanization Recipe**

| Ingredients | Concentration (phr) |
|---|---|
| Squalene | 100 |
| CBS | 1.2 |
| Sulfur | 2 |
| ZnO or $Zn_{1-x}Mg_xO$ | 5 |
| Stearic acid | 2 |

sample is isothermally annealed for 1 h at this temperature.

$Zn_{1-x}Mg_xO$ nanoparticles with different magnesium content, in the range of $0.13 < x < 0.24$ in weight, were prepared.

### Characterization of zinc/magnesium oxide ($Zn_{1-x}Mg_xO$) nanoparticles

Scanning electron microscope (Jeol JSM-5310), along with energy dispersive spectroscopy, was used to measure the magnesium and zinc content in the mixed metal oxide. X-Ray diffraction (Philips X'Pert) was used to characterize the crystal structure of $Zn_{1-x}Mg_xO$. The data obtained was refined with CELREF (The software is available free of charge at the Collaborative Computational Project Number 14 webpage)[20] to determine the lattice parameters of $Zn_{1-x}Mg_xO$. In this study, Zetasizer Nano ZS™ (Malvern Instruments) was used to measure the particle size of the $Zn_{1-x}Mg_xO$ particles.

### Model compound vulcanization

Model compound vulcanization with squalene as a model molecule for natural rubber has been chosen to study the role of the mixed metal oxide along the reaction using CBS as accelerator. The basic vulcanization recipe is given in Table I.

The work was performed using the same concentration of ZnO and $Zn_{1-x}Mg_xO$, 5 phr. The reaction for all formulations (containing ZnO or $Zn_{1-x}Mg_xO$) was performed in a preheated thermostatic oil bath at 140°C for 60 min. The vulcanization reaction is carried out in different vessels under nitrogen environment to avoid the oxidation of the double bonds of squalene. The model mixtures are continuously stirred to assure its homogeneity. During the reaction, vessels are taken from the oil bath at different preset times and quickly cold quenched in dried ice to stop the reaction. After cooling, the vessels were covered to avoid any UV influence, and stored in a refrigerator.

All vulcanizates were characterized by two analytical methods of HPLC coupled to an UV detector to cover both aspects of the vulcanization process: the fading of the accelerator and the formation of crosslinks between the model molecules. 0.1 g of the cold quenched vulcanized mixture were dissolved for 5 min in an ultrasonic bath at room temperature in 5 mL acetonitrile or a mixture of acetonitrile/2-propanol/*n*-hexane (72 : 17 : 11), depending on whether the accelerator evolution or the crosslink formation is investigated. Before injection, samples were filtered with a 0.45-μm Nylon filter to remove insoluble particles that would damage the column.

A VWR International LaChrom Elite High-Performance Liquid Chromatograph has been used. Data acquisition and treatment has been made using EZ Chrom Elite. To follow the accelerator evolution, the ultraviolet detector was set to 254 nm, and the mobile phase was an isocratic mixture of acetonitrile (HPLC quality) and water in proportion 90 : 10. When investigating the crosslink formation, the ultraviolet detector was set to 230 nm and the mobile phase was an isocratic mixture of acetonitrile, 2-propanol, and *n*-hexane (all HPLC quality) in proportion 72 : 17 : 11. In both cases, the flux was set to 1 mL/min, the injected volume was 20 μL, and the total time of the chromatogram was 15 min. A Teknokroma Kromasil 100 C-18 (5 μm, 15 cm × 0.4 cm) column has been used.

The identification of the different compounds was carried out earlier in our research group using different techniques.[17,21–25]

## RESULTS AND DISCUSSION

### Synthesis and characterization of $Zn_{1-x}Mg_xO$ nanoparticles

Table II summarizes the results achieved in the synthesis. It can be seen that in all syntheses the theoretical magnesium ($x_T$) content is lower than the actual value achieved ($x$). This higher magnesium content may be caused by the losses of material that occur during the precipitation and redissolution cycles. In the synthesis, poly(acrylic acid) and zinc nitrate are firstly dissolved in water and then purified by precipitation with acetone. This material is then dissolved again in water to be mixed afterwards with magnesium nitrate. During the first purification, where only zinc and not magnesium is present, part of the material could not be recovered

**TABLE II**
**Theoretical, $x_T$, and Actual, $x$, Magnesium Content, and Particle Size for the Different Samples of $Zn_{1-x}Mg_xO$**

| | $x_T$ | $x$ | $d_p$ (nm) |
|---|---|---|---|
| Sample I | 0.14 | 0.19 | 154 ± 35 |
| Sample II | 0.14 | 0.22 | – |
| Sample III | 0.07 | 0.14 | 106 ± 17 |
| Sample IV | 0.20 | 0.24 | 147 ± 32 |
| Sample V | 0.13 | 0.20 | 172 ± 12 |

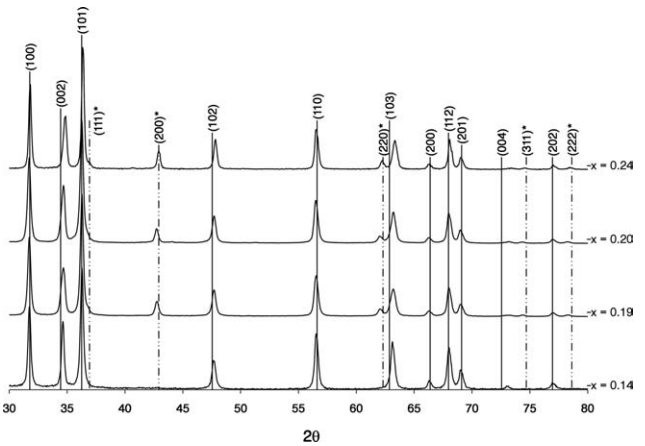


**Figure 1** XRD patterns of $Zn_{1-x}Mg_xO$.

and, subsequently, the final content of magnesium is slightly higher than expected.

Dynamic light scattering was used to measure the particle size of the $Zn_{1-x}Mg_xO$ particles. The results obtained are displayed in Table II. It can be seen that particle size is in the range of 106–172 nm. There is no apparent dependence of the particle size with the magnesium content.

X-ray diffraction was used to characterize the crystal structure of the mixed metal oxide particles. Figure 1 shows the X-ray diffraction patterns of the oxide products obtained in the different syntheses.

The patterns of the pure ZnO are indexed according to the known hexagonal phase (zincite),[26] and that of MgO is indexed according to its cubic phase (periclase).[27] In Figure 1, the vertical lines correspond to the standard reflections of the ZnO phase and the dashed vertical lines are the standard reflections of the MgO phase. The MgO planes are indicated with a star. The scans showed a weak (2 0 0) reflection of the MgO phase for all samples which indicates that the material is mostly present in the hexagonal phase (zincite) and that magnesium has been incorporated into the ZnO structure.

It can be seen in Figure 1 that when $x < 0.19$ no cubic phase is visible, only the zincite phase is present. This denotes that all magnesium has been integrated in the ZnO phase. At higher magnesium content, $0.19 \leq x \leq 0.24$, a weak (2 0 0) peak characteristic of the cubic MgO phase appeared. This indicates the coexistence of the two phases, zincite and periclase, although the intensity of the peaks implies that the majority of the material was in the form of zincite.

The magnesium content at which the (2 0 0) and (2 2 0) diffraction peaks of the MgO cubic phase appears seems be lower than the values reported on the literature. Geng *et al*.[28] found that for $x < 0.25$, only metastable $Zn_{1-x}Mg_xO$ was formed and Wang[29] reported a value of $x \leq 0.30$. Ohtomo *et al*.[30] and Zhang *et al*.[31] obtained that no cubic phase was formed if the magnesium content was lower than 33 and 39%, respectively. These results could be due to the different preparation methods used and the adhesion to the substrate in the laser deposited films or in the thin films grown by metal-organic chemical vapor deposition. Furthermore, there are small differences with the results reported by other authors using the same method.[19] These authors obtained that the cubic phase was formed if the magnesium content was higher than 21%. These deviations could be caused by variations in the calcination process such as the air flow in the oven and the amount of powder annealed. In addition, it is worth noting that no data was reported for the range of $0.12 \leq x \leq 0.21$.

It can be seen in Figure 1 that the diffraction peaks (0 0 2), (1 0 2), and (1 0 3) have shifted to higher diffraction angles compared to those of the hexagonal structure of ZnO.[26] These shifts are caused by the substitution of Zn atoms by Mg atoms in the hexagonal phase and lead to a decrease of the *c*-axis lattice constant.[19,28–33] This can be seen in Figure 2, where the dependence of $Zn_{1-x}Mg_xO$ lattice parameters of the hexagonal phase on Mg concentration is shown. The data were refined by CELREF.[20] As magnesium replaces zinc in the hexagonal phase, due to the smaller radius of $Mg^{2+}$ (0.57 Å) than that of $Zn^{2+}$ (0.60 Å), there is a shrinking of the lattice constant along the *c*-axis and a displacement of the diffraction peaks to higher angles.

Figure 2 shows that, despite the fact that the c-axis lattice constant shrinks as Mg incorporates into the structure, the *a*-axis lattice constant increases. These findings differ from the values reported by other researchers,[29] but it should be noted that the variation from the standard value of ZnO cell parameters' is very small. Nevertheless, there is almost no influence of the magnesium content which agrees with other authors.[19,30]

Figure 1 also shows that the diffraction peaks (2 0 0) and (2 2 0) of some samples have shifted to

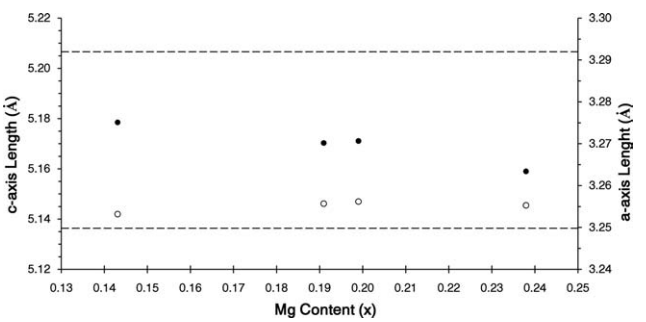


**Figure 2** Variation of $Zn_{1-x}Mg_xO$ hexagonal phase lattice constant *a* (open circle) and *c* (filled circle) with magnesium concentration *x*. The two dashed lines indicate the standard values of ZnO cell parameters.

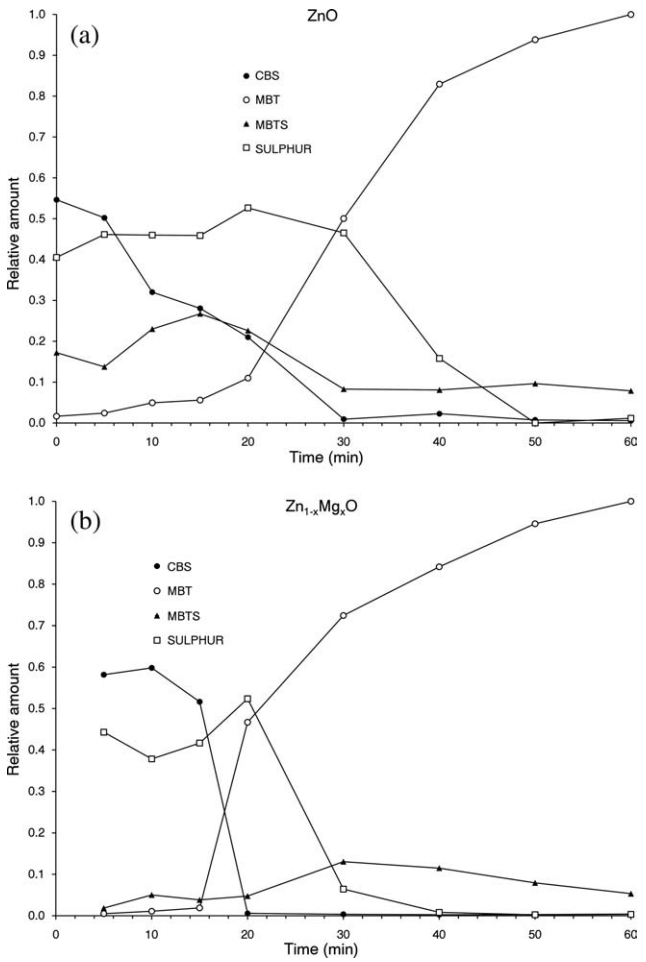


**Figure 3** Relative amount of major compounds as a function of reaction time during squalene vulcanisation with sulfur and CBS at 140°C using (a) ZnO and (b) $Zn_{1-x}Mg_xO$ as activator.

smaller diffraction angles compared to those of the cubic structure of MgO.[27] This is due to the incorporation of zinc into the MgO cubic phase. Note that there is no cubic phase when $x = 0.14$, indicating that all magnesium used in the synthesis of sample *I* has been incorporated in the zincite.

In summary, it has been demonstrated that by a polymer-based method it is feasible to obtain $Zn_{1-x}Mg_xO$ particles. The results obtained indicate that the appearance of the cubic phase occurs when the magnesium content is 19%, which is lower than other values reported in the literature.

In the light of the results obtained, sample IV was chosen to perform the model compound vulcanization reactions to test the activator character of the mixed metal oxide nanoparticles in accelerated sulfur vulcanization. This sample has a particle size of 147 nm, a magnesium content of 24%, and the XRD pattern has shown that almost all magnesium is incorporated into the zinc oxide structure. Although there is a weak reflection of the MgO phase, in Figure 1 there are no differences in the intensity of this phase when the magnesium content is between $0.19 \leq x \leq 0.24$. Furthermore, Figure 2 shows that the *c*-axis lattice constant of this sample is the lowest of all samples. These results indicate that sample IV has incorporated more magnesium into the ZnO structure than any other sample.

### $Zn_{1-x}Mg_xO$ nanoparticles as new activators for vulcanization

Model compound vulcanization with squalene as a model molecule for natural rubber has been chosen to study the role of the mixed metal oxide along the reaction using CBS as accelerator. The basic vulcanization recipe has been shown in Table I.

The evolution of CBS, 2-mercaptobenzothiazole (MBT), 2,2′-bisbenzothiazole disulphide (MBTS), and sulfur when using ZnO and $Zn_{1-x}Mg_xO$ as activators is shown in Figure 3. From Figure 3, it can be established some differences that occur when the new activator is used. $Zn_{1-x}Mg_xO$ nanoparticles provoke a faster consumption of CBS and sulfur, while in the case of ZnO it occurs in a more gradual manner.

The breakdown of the accelerator is one of the most used parameters to study what occurs during the scorch time since it has been demonstrated to be the bottle neck that determines the length of the scorch time.[15] In the case of acceleration by benzothiazolesulphenamides, the accelerator is depleted autocatalytically with the formation of 2-mercaptobenzothiazole.[34] The MBT formed from the breakdown of CBS react with CBS to form the active sulfurating agents and the rate of the CBS depletion's is about proportional to the amount of MBT present.

Figure 4 shows the CBS concentration in the samples with ZnO (empty circle) and with $Zn_{1-x}Mg_xO$

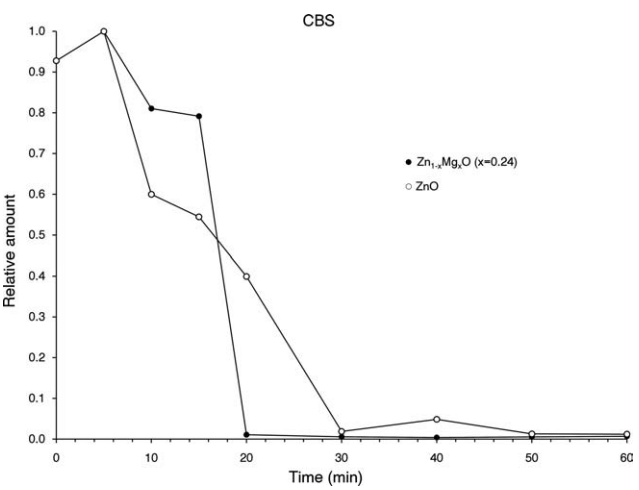


**Figure 4** Breakdown of CBS as a function of the reaction time with $Zn_{1-x}Mg_xO$ and ZnO as activator.

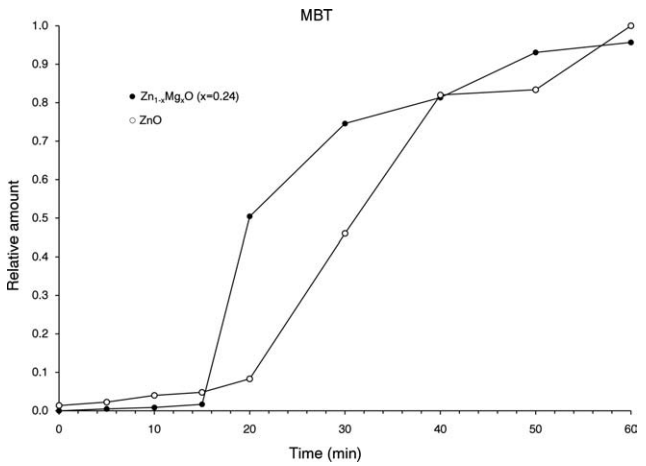


**Figure 5** MBT concentration as a function of the reaction time with $Zn_{1-x}Mg_xO$ and ZnO as activator.

(filled circle) as a function of the reaction time. It can clearly be seen that the utilization of ZnO or $Zn_{1-x}Mg_xO$ as activators influences the breakdown of CBS differently. When $Zn_{1-x}Mg_xO$ nanoparticles are used, CBS is completely degraded after 20 min while, with standard ZnO, there is around 40% of unreacted CBS which does not disappear entirely until 30 min as reported earlier.[3,15-17,21] It can be seen that the breakdown of the accelerator does not commence very differently when using $Zn_{1-x}Mg_xO$ or zinc oxide but that the mixed metal oxide provokes a much faster disappearance of CBS.

Furthermore, it is interesting to study the decomposition of the accelerator with respect to the evolution of sulfur and MBT to understand the reactions taking place during the scorch time and before the crosslink formation. Decomposition of the accelerator and transformation of the crosslink precursor into a crosslink yields to MBT.

As it can be seen in Figure 5, $Zn_{1-x}Mg_xO$ nanoparticles lead to higher amounts of MBT at shorter reaction times. Since MBT is a decomposition product of the accelerator and the breakdown of the accelerator occurs faster when the activator are the mixed metal oxide nanoparticles, it is not surprising to observe that the formation of MBT is more rapidly with $Zn_{1-x}Mg_xO$ than zinc oxide.

Figure 6 shows that the consumption of sulfur occurs faster when $Zn_{1-x}Mg_xO$ nanoparticles are used as the accelerator. At 30 min it has almost disappeared. For standard ZnO, it is not until 50 min when it has been totally consumed. Furthermore, the fading of sulfur with $Zn_{1-x}Mg_xO$ is faster compared with the values that have been reported before with MgO.[15,35]

Previous researchers have described that, when ZnO is substituted by MgO, CBS is dissociated very rapidly and that MgO produces higher amount of MBT at shorter reaction times.[15] It has been proposed that the quicker dissociation of the accelerator is most likely to occur due to less complex formation between the magnesium ions and MBT occurs.[16]

Another explanation to this behavior has been postulated by our research group. Díaz[35] performed MCV studies with MgO as activator using squalene and squalane, a saturated form of squalene, in the presence or absence of sulfur. It was found that when sulfur was not present in the reaction mixture, the breakdown of the accelerator is much slower and not complete after 60 min of reaction time. From these results, it was concluded that the dissociation of CBS occurs via sulfur activation from magnesium oxide.

The fact that $Zn_{1-x}Mg_xO$ nanoparticles dissociate CBS faster and produce higher amounts of MBT at shorter reaction times means that the CBS dissociation occurs by a different mechanism than with zinc

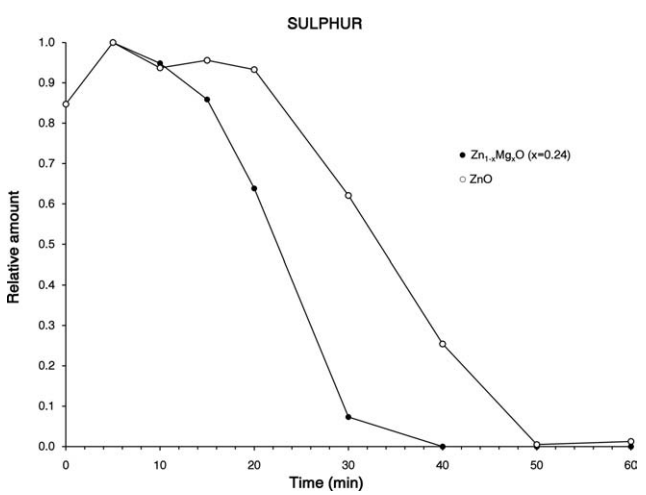


**Figure 6** Degradation of sulfur during vulcanization with standard ZnO and $Zn_{1-x}Mg_xO$.

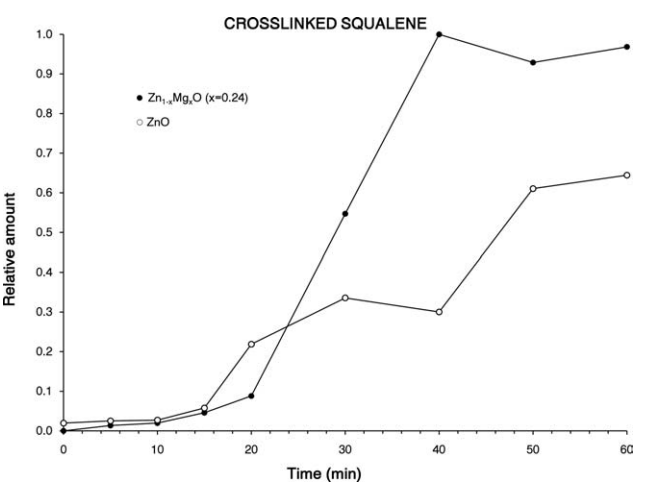


**Figure 7** Evolution of total crosslinked squalene during vulcanization with standard ZnO and $Zn_{1-x}Mg_xO$.

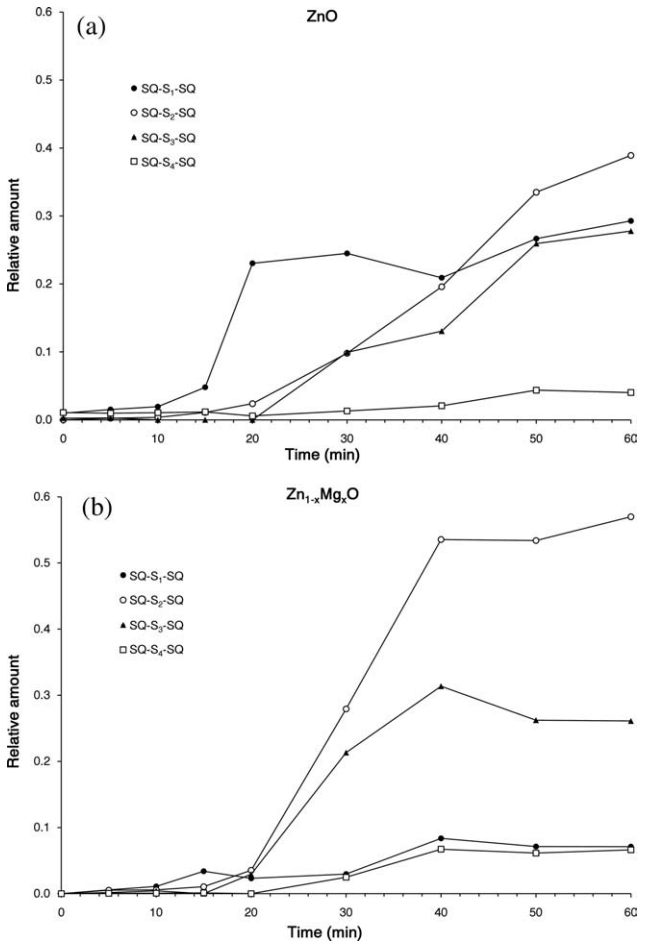


**Figure 8** Relative amount of crosslinked products as a function of reaction time during squalene vulcanization with sulfur and CBS at 140°C using (a) ZnO and (b) $Zn_{1-x}Mg_xO$ as activator.

oxide. Since the breakdown of the accelerator and the formation of MBT with $Zn_{1-x}Mg_xO$ is more similar to the manner that occurs when MgO is used,[15,16,35] it can be deduced that the presence of magnesium into the zinc oxide structure alter ZnO performance. Furthermore, the consumption of sulfur takes place faster with $Zn_{1-x}Mg_xO$ than with ZnO or MgO indicating that $Zn_{1-x}Mg_xO$ nanoparticles provoke a faster reaction of sulfur with the accelerator.

The evolution of crosslinked squalene during vulcanisation with ZnO or $Zn_{1-x}Mg_xO$ as activator is shown in Figure 7. It can be noted that even though the formation of crosslinked squalene commences later when $Zn_{1-x}Mg_xO$ nanoparticles are used, a higher crosslink degree, calculated as the total amount of crosslinked squalene formed, is attained. These findings are in agreement with the results reported before. Chapman[8] found that when high surface area/small-particle size zinc oxides were used scorch delay was increased a little; and Parasiewicz and coworkers[7] found that the use of ZnO nanoparticles resulted in a slightly longer scorch time.

Regarding the crosslink degree achieved, it is worth noting that mixed metal oxide nanoparticles lead to around a 30% higher crosslink degree than the one obtained with standard zinc oxide. This effect can be partly attributed to the small particle size of the $Zn_{1-x}Mg_xO$ particles. Bhowmick and coworkers[4,5] found that ZnO nanoparticles (30–70 nm) increased the crosslink degree by 15% compared with standard ZnO. On the other hand, the fact that, even with bigger sizes, higher amounts of crosslinked products are formed suggests that $Zn_{1-x}Mg_xO$ nanoparticles are more active and more effective transporting sulfur into the hydrocarbon chain than ZnO nanoparticles.

As stated earlier, when MgO is used as activator the accelerator is dissociated very rapidly and a large quantity of intermediate compounds are formed but its main drawback is the low reticulation degree achieved.[15,16] The fact that the breakdown of the accelerator and the consumption of sulfur occur faster but crosslinked products appear later, indicate that larger amounts of intermediate compounds that are active sulfurating species are produced when the activator is $Zn_{1-x}Mg_xO$.

Concerning the crosslink structure, some changes were detected when working with $Zn_{1-x}Mg_xO$ in comparison with ZnO as it has been pointed out in previous sections. Figure 8 shows the evolution of the different crosslinked products formed: mono- (Sq-*S*-Sq), di- (Sq-$S_2$-Sq), tri- (Sq-$S_3$-Sq), and tetrasulphidic (Sq-$S_4$-Sq) crosslinks. $Zn_{1-x}Mg_xO$ nanoparticles provoke that the major crosslinked products formed are disulphidic crosslinks and that very little amount of monosulphidic crosslinks are produced. It can be seen that the formation of the monosulphidic crosslinks starts at shorter reaction times when ZnO

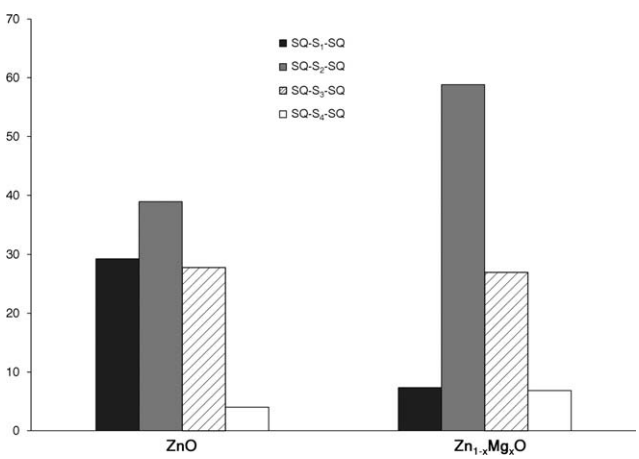


**Figure 9** Distribution of sulfidic crosslinks (crosslink structure) in 60 min vulcanizates with standard ZnO and $Zn_{1-x}Mg_xO$.

is used but in both cases the major crosslinked product obtained is Sq-$S_2$-Sq.

Figure 9 shows the percentage of mono-, di-, tri-, and tetrasulphidic crosslinks in the different samples tested. The main effect of the mixed metal oxide seems to be the decrease of monosulphidic crosslinks by an increase in the formation of disulphidic crosslinks. However, the proportion of tri- and tetrasulphidic crosslinks is not altered by the use of $Zn_{1-x}Mg_xO$ nanoparticles as activator.

In summary, the results obtained have shown that it is possible to take advantage of the behavior of both ZnO and MgO in sulfur vulcanization with $Zn_{1-x}Mg_xO$ nanoparticles. It has been seen that the reactions that take place during the scorch time, the breakdown of the accelerator and the formation of MBT, occur faster; fact that could be due to the presence of magnesium into the zinc oxide structure.

On the other hand, the formation of the crosslinks start at longer reaction times, feature reported by other authors using zinc oxide nanoparticles. Nevertheless, the crosslink degree achieved is higher than those obtained with zinc oxide nanoparticles. Furthermore, the mixture of ZnO and MgO shows a crosslink degree similar to the one obtained with magnesium oxide. Therefore, $Zn_{1-x}Mg_xO$ nanoparticles not only overcome the disadvantages of the mixture of ZnO and MgO but a better performance is achieved.

Moreover, the use of $Zn_{1-x}Mg_xO$ nanoparticles as activator lead to a reduction of the total amount of zinc used in rubber compounds due to the presence of magnesium into the zinc oxide structure. This characteristic could minimize the environmental effect of rubber compounds, which is a major concern in the rubber industry.

## CONCLUSIONS

Mixed metal oxides nanoparticles of zinc and magnesium with different magnesium content have been synthesized with a particle size in the range of 95–172 nm. The X-ray diffraction patterns have proved that magnesium atoms incorporate into the zinc oxide structure altering the lattice parameters.

When the magnesium content of the mixed metal oxide is below 19% only the metastable phase $Zn_{1-x}Mg_xO$ (modified zincite) is formed. At higher magnesium content, the cubic phase appeared indicating the coexistence of the two phases. Despite that, the intensity of the cubic phase denotes that the majority of the material is in the form of modified zincite.

Model compound vulcanization with squalene has been carried out to study the role of the mixed metal oxide along the reaction using CBS as accelerator. Concerning the reactions that take place during scorch time, it has been proved that the presence of magnesium into the zinc oxide structure modifies the manner that ZnO performs. The breakdown of the accelerator and the formation of MBT are faster with $Zn_{1-x}Mg_xO$ and more similar to the manner that occurs when MgO is used. The consumption of sulfur takes place faster with $Zn_{1-x}Mg_xO$ than with ZnO or MgO.

The formation of crosslinked squalene commences later when $Zn_{1-x}Mg_xO$ nanoparticles are used but a 30% higher crosslink degree is attained. These results prove that $Zn_{1-x}Mg_xO$ nanoparticles are more active and more effective transporting sulfur into the hydrocarbon chain than ZnO.

Regarding the crosslink structure, the mixed metal oxide produces a decrease of monosulphidic crosslinks and an increase of disulphidic crosslinks. The proportion of tri- and tetrasulphidic crosslinks is not altered by the use of $Zn_{1-x}Mg_xO$ nanoparticles as activator.

In summary, the use of $Zn_{1-x}Mg_xO$ nanoparticles as activator leads to a reduction of the total amount of zinc used in rubber compounds which would reduce the environmental impact of the rubber industry.

## References


1. Walter, J. Tire Technology International; Ukip Media Events: Willenhall, UK, 2009; p 18.
2. Heideman, G.; Datta, R. N.; Noordermeer, J. W. M. Rubber Chem Technol 2004, 77, 512.
3. Borrós, S.; Agulló, N. Kautschuk Gummi Kunststoffe 53, 131, 2000.
4. Sahoo, S.; Kar, S.; Ganguly, A.; Maiti, M.; Bhowmick, A. K. Polym Polym Compos 2008, 16, 193.
5. Sahoo, S.; Maiti, M.; Ganguly, A.; George, J. J.; Bhowmick, A. K. J Appl Polym Sci 2007, 105, 2407.
6. Begum, P. M. S.; Joseph, R.; Yusuff, K. K. M. Progr Rubber Plast Recycling Technol 2008, 24, 141.
7. Pysklo, L.; Pawlowski, P.; Parasiewicz, W.; Slusarski, L. Kautschuk Gummi Kunststoffe 2007, 60, 548.
8. Chapman, A. V. In IRC 2005, Maastricht: 2005.
9. Heideman, G.; Datta, R. N.; Noordermeer, J. W. M.; van Baarle, B. J Appl Polym Sci 2005, 95, 1388.
10. Pysklo, L.; Pawlowski, P.; Nicinski, K.; Slusarski, L.; Wlodarska, M.; Bak, G. Kautschuk Gummi Kunststoffe 2008, 61, 442.
11. Henning, S. K. In Fall 172nd Technical Meeting of Rubber Division; American Chemical Society, Rubber Division: Akron, OH, 2007.
12. Heideman, G.; Noordermeer, J. W. M.; Datta, R. N.; van Baarle, B. Kautschuk Gummi Kunststoffe 2003, 56, 650.
13. Heideman, G.; Noordermeer, J. W. M.; Datta, R. N.; van Baarle, B. Macromol Symp 2006, 245–246, 657.
14. Heideman, G.; Noordermeer, J. W. M.; Datta, R. N.; Van Baarle, B. Rubber Chem Technol 2005, 78, 245.
15. Garreta, E.; Agulló, N.; Borrós, S. Kautschuk Gummi Kunststoffe 2005, 55, 82.
16. Heideman, G.; Noordermeer, J. W. M.; Datta, R. N.; van Baarle, B. Kautschuk Gummi Kunststoffe 2005, 58, 30.
17. Vega, B.; Agulló, N.; Borrós, S. Rubber Chem Technol 2008, 80, 739.
18. Vega, B. PhD Thesis, Universitat Ramon Llul: Barcelona, 2008.
19. Lu, G.; Lieberwirth, I.; Wegner, G. J Am Chem Soc 2006, 128, 15445.

20. www.ccp14.ac.uk/ccp/web-mirrors/lmgp-laugier-bochu/.
21. Vidal-Escales, E.; Borrós, S. Talanta 2004, 62, 539.
22. Rodríguez, S.; Masalles, C.; Agulló, N.; Borrós, S.; Comellas, L.; Broto, F. Kautschuk Gummi Kunststoffe 1999, 52, 438.
23. Folch, I.; Borrós, S.; Amabilino, D. B.; Veciana, J. J Mass Spectrometry 2000, 35, 550.
24. Gros, M.; Borrós, S.; Amabilino, D. B.; Veciana, J.; Folch, I. J Mass Spectrometry 2001, 36, 294.
25. Borrós, S.; Vidal-Escales, E.; Agulló, N.; Van Ooij, W. J. Kautschuk Gummi Kunststoffe 2000, 53, 711.
26. Joint Committee on Powder Diffraction Standards Diffraction Data File, JCPDS International Center for Diffraction Card No. 36-1451.
27. Joint Committee on Powder Diffraction Standards Diffraction Data File, JCPDS International Center for Diffraction Card No. 45-0946.
28. Geng, W.; Li, N.; Li, X.; Lai, X.; Wang, L.; Long, B.; Ning, J.; Tu, J.; Qiu, S. Mater Res Bull 2008, 43, 601.
29. Wang, Y. S. J Crystal Growth 2007, 304, 393.
30. Ohtomo, A.; Kawasaki, M.; Koida, T.; Masubuchi, K.; Koinuma, H.; Sakurai, Y.; Yoshida, Y.; Yasuda, T.; Segawa, Y. Appl Phys Lett 1998, 72, 2466.
31. Zhang, Y.; Du, G.; Liu, D.; Zhu, H.; Cui, Y.; Dong, X.; Yang, S. J Crystal Growth 2004, 168, 140.
32. Vashaei, Z.; Minegishi, T.; Yao, T. J Crystal Growth 2007, 306, 269.
33. Chawla, S.; Jayanthi, K.; Chander, H.; Haranath, D.; Halder, S. K.; Kar, M. J Alloys Compounds 2008, 459, 457.
34. Mark, J. E.; Erman, B.; Eirich, F. R. Science and Technology of Rubber; Academic Press: San Diego, 1994.
35. Díaz, M. Master Thesis, Universitat Ramon Llull: Barcelona, 2001.